Available online at www.sciencedirect.com
ScienceDirect
Trans. Nonferrous Met. Soc. China 23(2013) 2060−2065
Transactions of Nonferrous Metals Society of China
www.tnmsc.cn

Effect of germanium on electrochemical performance of chain-like Co−P anode material for Ni/Co rechargeable batteries

Jia-jia LI[1], Xiang-yu ZHAO[1], Wei DU[1], Meng YANG[1], Li-qun MA[1], Yi DING[1], Xiao-dong SHEN[1,2]

1. College of Materials Science and Engineering, Nanjing University of Technology, Nanjing 210009, China;
2. State Key Laboratory of Materials-Oriented Chemical Engineering, Nanjing University of Technology, Nanjing 210009, China

Received 15 May 2012; accepted 14 May 2013

Abstract: Co−P (4.9% P) powders with a chain-like morphology were prepared by a novel chemical reduction method. The Co−P and germanium powders were mixed at various mass ratios to form Co−P composite electrodes. Charge and discharge test and electrochemical impedance spectroscopy (EIS) were carried out to investigate the electrochemical performance, which can be significantly improved by the addition of germanium. For instance, when the mass ratio of Co−P powders to germanium is 5:1, the sample electrode shows a reversible discharge capacity of 350.3 mA·h/g and a high capacity retention rate of 95.9% after 50 cycles. The results of cyclic voltammmetry (CV) show the reaction mechanism of $Co/Co(OH)_2$ within Co−P composite electrodes and EIS indicates that this electrode shows a low charge-transfer resistance, facilitating the oxidation of Co to $Co(OH)_2$.
Key words: Co−P alloy; germanium; anode material; electrochemical performance

1 Introduction

Some traditional Ni-based alkaline rechargeable batteries have been well studied, such as nickel/cadmium (Ni/Cd), nickel/iron(Ni/Fe), nickel/zinc(Ni/Zn), and nickel/metal hydride(Ni/MH) batteries [1,2]. However, practical application of these batteries was limited by drawbacks of toxicity, low capacity, and/or poor cycling stability [3,4]. In recent years, considerable research attention has been paid to Ni/Co alkaline rechargeable batteries as a promising entry to the energy storage electrode materials for their several advantages: cycle stability, discharge capacity, enhancement of electrode conductivity, charging efficiency, and suppression of electrode swelling during charge and discharge cycling [5−8].

The negative materials of Ni/Co alkaline rechargeable batteries could be composed of Co powders, Co-based alloys or cobalt oxides [9−12]. The Co powders had a high discharge capacity. ZHAO et al [9] studied the electrochemical properties of crystalline Co powders and found that their maximum discharge capacity was about 364 mA·h/g. In addition, CHUNG et al [10,11] found that the discharge capacity of crystalline Co powders could reach more than 400 mA·h/g. But the expensive price of Co powders limited their practical application in Ni/Co batteries. LI et al [12] found that the discharge capacity of mesoporous nano-Co_3O_4 could reach 436.5 mA·h/g and still remained at 351.5 mA·h/g after 100 cycles. Up to now, some researchers have paid more attention to binary Co-based alloys, which are mainly made up of Co−B [13−16], Co−Si [17], Co−S [18,19] and Co−P [20] alloys. They reported that chemical reduction method was beneficial to achieve fine particles and thus good electrochemical performance. But this aspect for Co−P powders was not reported, which may be attributed to a high energy barrier of the reduction reaction. HARAN et al [20] and DURAIRAJAN et al [21] reported that Co−P coating could improve the discharge capacity and cycle stability of hydrogen storage alloys. Afterwards, CAO et al [22]

Foundation item: Project supported by the Priority Academic Program Development of Jiangsu Higher Education Institutions of China; Project (CXLX11_0359) supported by Research Innovative Projects for Average College Graduate Students of 2011 in Jiangsu Province, China; Project (RERU 2011010) supported by Open Subject of State Key Laboratory of Rare Earth Resource Utilization, China; Project (51201089) supported by the National Natural Science Foundation of China; Project (CPSF 2012M521064) supported by China Postdoctoral Science Foundation
Corresponding author: Li-qun MA; Tel: +86-25-83587243; E-mail: maliqun@njut.edu.cn
DOI: 10.1016/S1003-6326(13)62696-5

synthesized Co−P alloy powders by ball milling and reported that they showed a stable discharge capacity of about 300 mA·h/g, but poor activation property. Recently, PENG et al [23] used a solid sintering method to prepare Co_2P material, which exhibited a maximum discharge capacity of 223.5 mA·h/g and a high capacity retention rate of 97.9% after 300 cycles in Ni/Co batteries. All these indicated that nonmetal elements (B, S, P, Si) had catalytic effect on Co electrodes. Germanium and silicon are in the same main group, therefore, germanium has a certain degree catalytic effect like silicon on Co electrodes. On the other hand, germanium as a mental element was first to be added into the Co-based electrodes.

In this work, Co−P powders were prepared using a novel chemical reduction method and the electrochemical performance of Ni/Co batteries was investigated. The effect of the addition of germanium powders into the Co−P electrodes was also studied.

2 Experimental

All the reagents were of analytical grade. The Co−P powders were synthesized as follows. 10.1 g $CoSO_4·7H_2O$, 10.6 g $Na_3C_6H_5O_7·2H_2O$, 19.8 g $(NH_4)_2SO_4$ and 11.4 g $NaH_2PO_2·H_2O$ were successively dissolved in distilled water to form 300 mL aqueous solution, which was then heated to 90 °C in water bath and adjusted to pH 9 with $NH_3·H_2O$ solution. Afterwards, 20 mL $PdCl_2$ solution (0.5 g/L) as initiator was added into the resulting mixture with constant stirring. A black precipitate was thoroughly rinsed with distilled water and ethanol. Finally, the sample was dried in a vacuum at 60 °C for 12 h.

The structure of the powders was studied by XRD in a Thermo ARL X' TRA diffractometer, equipped with Cu K_α radiation. The morphology of the powders was analyzed by a JSM−5610LV scanning electron microscope. Chemical composition of the prepared sample was determined by inductivity coupled plasma atomic emission spectroscopy (ICP-AES, Optima2000, Thermo Electron).

The as-prepared Co−P powders were mixed with germanium powders (≥99% purity, 25 μm) in a mortar at the mass ratios of 1:0, 1:1, 3:1, and 5:1 to form various mixtures, which were signed as A, B, C and D in the following section, respectively. Work electrodes, in a half-cell consisting of a $Ni(OH)_2$/NiOOH counter electrode and a Hg/HgO reference electrode under a 6 mol/L KOH solution, were constructed by pressing 0.1 g active powders and 0.3 g carbonyl nickel powders into a pellet with 10 mm in diameter and 0.6−0.8 mm in thickness, under a pressure of 15 MPa.

The work electrode was charged at 100 mA/g for 6 h, followed by a 10 min rest and then discharged at 300 mA/g to the cut-off potential of −0.6 V (vs. Hg/HgO) using BT−2000 testing equipment (Arbin, USA). Electrochemical impedance spectroscopy (EIS) of the electrodes was obtained in the frequency ranging from 100 kHz to 1 mHz with an amplitude of 5 mV at 50% depth of discharge (DOD). Cyclic voltammetry (CV) was carried out at a sweep rate of 0.1 mV/s from −1.2 to −0.4 V (vs Hg/HgO). All the electrochemical tests were performed on a CHI 660D electrochemical workstation in the 6 mol/L KOH solution at 298 K.

3 Results and discussion

3.1 Structure and morphology of Co−P particles

Figure 1 shows the SEM images of the as-prepared Co−P alloy powders, which present a chain-like morphology arrayed by Co−P particles with a size of about 1 μm. The XRD pattern of Co−P powders is shown in Fig. 2. It gives a few of weak diffraction lines, which

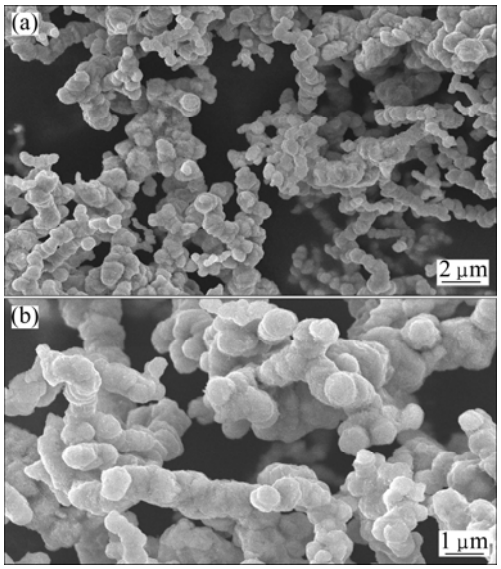

Fig. 1 SEM images of Co−P alloy

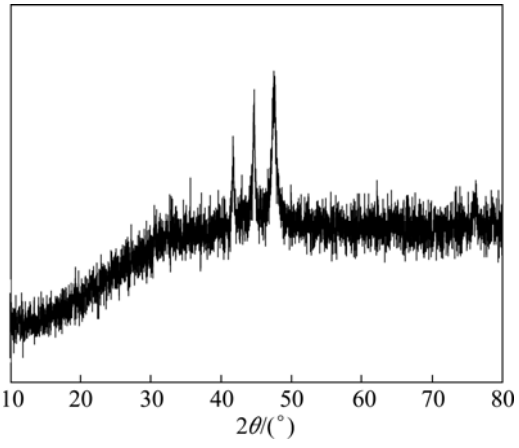

Fig. 2 XRD pattern of as-prepared Co−P alloy

can be indexed from the hexagonal Co structure (JCPDS 5—727). This indicates the existence of crystalline Co structure while separate phase of elemental phosphor cannot be found, which is in agreement with the XRD result by CAO et al [22]. The composition of the alloy obtained from the result of ICP-AES is $Co_{92.12}P_{7.88}$, which shows a phosphor content of 4.3%. So, the low content of phosphor may give rise to the outcome that phosphorus cannot be found in XRD pattern of Co−P alloy.

3.2 Effect of germanium on electrochemical performance of Co−P electrodes

Figure 3 shows cycle stability of the Co−P electrodes without and with the addition of germanium powders at a high discharge current density of 300 mA/g. It is clear that there is a sharp decrease in discharge capacity of all electrodes in initial fifteen cycles, which is due to the fact that a part of $Co(OH)_2$ accepts additional hydroxide ions to form the dark blue $Co(OH)_4^{2-}$ dicobaltite ion in the alkaline solution. Then the blue $Co(OH)_4^{2-}$ would react with oxygen in the electrolyte to form the brown CoOOH precipitate, which was an irreversible exsolution process [24]. After 15 cycles, the formation of a large amount of CoOOH may inhibit the exsolution process of $Co(OH)_2$ and redox of Co trends to a dynamic equilibrium process of a stable discharge capacity as shown in Fig. 3. Moreover, the discharge capacity of Co−P electrode without germanium can reach about 300 mA·h/g at the 50th cycle, which is similar to Co−P electrode prepared by ball milling [22]. However, the initial electrochemical discharge capacity of the milled Co−P electrode is less than 200 mA·h/g and must be fully activated in nearly 30 cycles [22]. On the contrary, the as-prepared Co−P electrode shows no activation process and a high discharge capacity of 552.2 mA·h/g in the first discharge cycle, which could be attributed to fine particles formed by the chemical reduction method. With the addition of germanium into the Co−P electrodes, the composite electrodes represent a notable increase in the discharge capacity. Compared with sample A, sample D shows a discharge capacity of 350.3 mA·h/g at the 50th cycle, 50 mA·h/g higher than sample A. In addition, sample D has a high reversible cycling capacity retention rate S_{50} (S_{50}=C_{50}/C_{15}×100%) of 95.9%.

The specific electrochemical discharge results are listed in Table 1. Sample D demonstrates the best discharge performance and best cycling stability. These results indicate that germanium has a catalytic effect on the electrochemical performance of the composite electrodes. To investigate the effect of germanium on Co−P powder, the cyclic voltammetry (CV) curves of samples A and D at the 30th cycle are shown in Fig. 4. Each curve consists of a pair of oxidation and reduction peaks. After addition of germanium, the shapes of the two CV curves are basically consistent, noting that no change of the electrochemical reaction mechanism appears after the addition of germanium. Furthermore, the anodic peak of electrode moves to more negative potential and the cathodic peak shifts left, indicating that with addition of germanium, reversible property of Co−P powders has been improved.

Table 1 Electrochemical data from discharge curves of electrodes

Electrode	C_1/ (mA·h·g^{-1})	C_{15}/ (mA·h·g^{-1})	C_{30}/ (mA·h·g^{-1})	C_{50}/ (mA·h·g^{-1})	S_{50}/ %
A	552.2	322.6	309.6	304.0	94.2
B	666.9	368.5	332.3	315.8	85.7
C	628.0	353.2	324.4	318.0	90.0
D	581.5	365.1	350.8	350.3	95.9

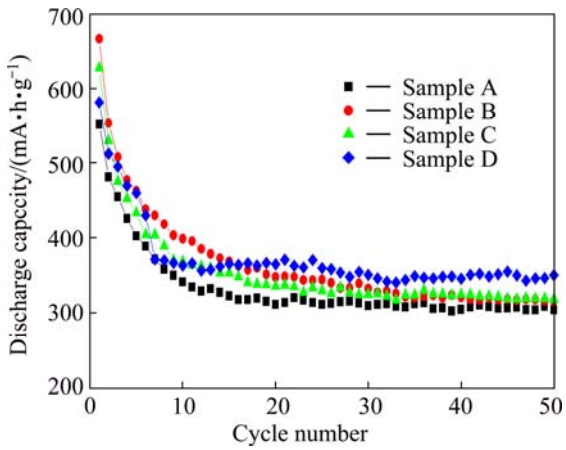

Fig. 3 Cycling stability of Co−P electrodes at high current rate of 300 mA/g

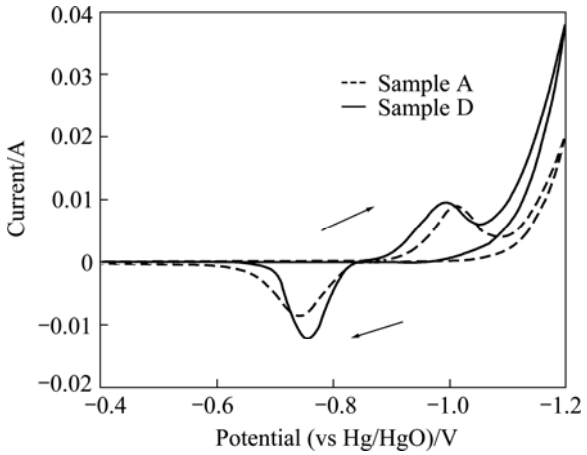

Fig. 4 Comparison of CV curves between electrodes A and D at scan rate of 0.1 mV/s

3.3 Electrochemical mechanism of germanium on Co−P electrodes

For better understanding the effect of germanium on the electrochemical performance of the composite electrodes, electrochemical impedance spectroscopy (EIS), as a nondestructive testing technology, was adopted to characterize the electrochemical processes of composite electrodes during charge and discharge testing. Figure 5 shows the EIS patterns of the electrodes at the 50% DOD at the 30th cycle. As shown in Nyquist plots of Fig. 5(a), there are three parts in the curve of electrode A, which is consistent with the Bode-phase plots including three time constants, as shown in Fig. 5(b). The semicircle in high frequency region reflects the contact resistance in the electrode A. The semicircle in subsequent is related to the charge-transfer resistance at the interface of electrode/electrolyte. In low frequency region, the pattern of the electrode A shows a slope line, which is caused by diffusion of soluble cobalt ions within electrode A. And the resistance related to the semicircle is the chord length to which the semicircle was corresponding [25]. Moreover, the EIS pattern of electrodes B, C or D only includes two parts, corresponding to contact resistance and charge-transfer resistance. The inset in Fig. 5(a) shows the equivalent circuit for EIS. R_1, R_2, and R_3 represent solution resistance, contact resistance and charge-transfer resistance, and specific resistances are listed in Table 2. The charge-transfer resistance of electrode B, C or D is less than that of electrode A, and electrode D shows the lowest charge-transfer resistance. The addition of germanium facilitates the oxidation of Co to $Co(OH)_2$ in the composite electrodes, resulting in a significant increase in discharge capacity.

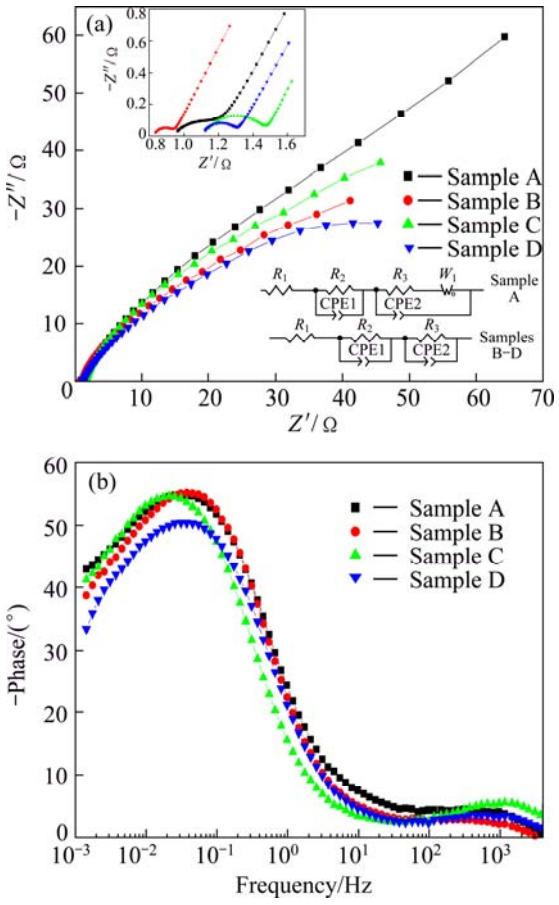

Fig. 5 EIS patterns of composite electrodes at 30th cycle of 50% DOD: (a)Nyquist plots; (b) Bode-phase plots

Table 2 Specific resistances of equivalent circuit for EIS

Electrode	R_1/(Ω·cm^2)	R_2/(Ω·cm^2)	R_3/(Ω·cm^2)
A	0.9365	0.2802	116.1
B	0.8247	0.1114	86.12
C	1.116	0.3554	106.6
D	1.105	0.1967	83.2

In order to further confirm the electrochemical reaction mechanism of electrode D, cyclic voltammetry (CV) curves of electrode D during the initial four cycles are presented in Fig. 6. It is observed that in the first discharge process, two oxidation peaks appear around at the potentials of −0.78 and −0.70 V, respectively. From the 2nd to the 4th CV cycles, the oxidation peak shifts to −0.76 V obviously. It is clear that there are two oxidation peaks only in the first cycle, and no reduction peak can be seen. So, the first peak is the oxidation of hydrogen adsorbed on the surface of electrode D. Usually, the oxidation peak potential of traditional hydrogen storage appears around −0.9 V [26] while that of electrode D at the first cycle occurs at −0.78 V. This may be attributed to the semiconductor property of germanium [27]. With addition of germanium, the polarization resistance of electrode D increases, as a result that hydrogen desorption potential changes from −0.90 V to −0.78 V. From the second cycle, the catalytic effect of germanium within electrode D is dominant and there is a pair of remarkable redox peaks, indicating that a reversible

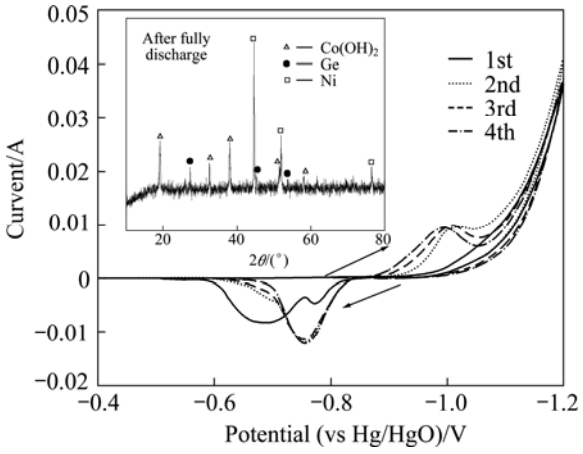

Fig. 6 CV curves of electrode D at scan rate of 0.1 mV/s

oxidation/reduction reaction exists. The shape and peak voltage of CV cycles are very similar to those of Co−B, Co−Si and Co−S alloys [16−18]. In addition, the XRD pattern of discharge products embedded in Fig. 6 confirms that the new phase $Co(OH)_2$ occurs on electrode D after discharge.

Hence, there is an irreversible reaction between phosphor and the alkaline solution, as that of B in Co−B alloy [28,29]. In initial cycles, phosphor on the surface dissolved in the alkaline solution sharply, resulting in more contact area between Co and alkaline solution to form $Co(OH)_2$. So, high discharge capacity is shown in Fig. 3 in initial cycles. And the discharge capacity of Co−P electrodes after adding a bit of germanium powder is increased, which indicates that germanium powders show catalytic effect on the reaction between electrode and electrolyte. As it can be seen, the sample D shows the best electrochemical discharge capacity of 350.3 mA·h/g at the 50th cycle, which is much more than that of sample A. There has been not any report about the catalytic effect of germanium at present. More investigations in this field may help to solve the problem.

Based on the above analysis, the reaction of the electrode D could be described as follows [30]:

$$Co+2OH^- \rightleftharpoons Co(OH)_2+2e \quad (1)$$

4 Conclusions

1) Among the materials, the sample D shows a discharge capacity of 350.3 mA·h/g at the 50th cycle and a high cycling capacity retention rate of 95.9%, indicating the best discharge performance and the best cycling stability, higher than that of as-prepared sample A.

2) The addition of germanium facilitates the charge-transfer process of the composite electrodes and promotes the redox reaction between Co and $Co(OH)_2$ within the composite electrodes.

References

[1] LINDEN D, REDDY T B. Handbook of batteries [M]. WANG Ji-qiang. Beijing: Chemical Industry Press, 2007: 487−658. (in Chinese)

[2] SHUKLA A K, VENUGOPALAN S, HARIPRAKASH B. Nickel-based rechargeable batteries [J]. J Power Sources, 2001, 100: 125−148.

[3] LAWRENCE H T, ALBERT H Z. Electrolyte management considerations in modern nickel/hydrogen and nickel/cadmium cell and battery designs [J]. J Power Sources, 1991, 63: 53−61.

[4] ZHANG Y Y, JIAO L F, YUAN H T, SONG D W, WANG Y J, ZHANG Y H. Effects of amorphous Co−C on the structural and electrochemical characteristics of $La_{0.8}Mg_{0.2}Ni_{0.8}Mn_{0.1}Co_{0.5}Al_{0.1}$ hydrogen storage alloy [J]. J Alloys Compd, 2009, 467: L16−L20.

[5] FENG Y, JIAO L F, YUAN H T, ZHAO M. Study on the preparation and electrochemical characteristics of MgNi−CoB alloys [J]. J Alloys Compd, 2007, 440: 304−308.

[6] SONG D W, WANG Y J, WANG Y P, JIAO L F, YUAN H T. Electrochemical hydrogen storage performance of AB_5-CoB composites synthesized by a simple mixing method [J]. Rare Metals, 2009, 28(6): 629−632.

[7] ZHAO X Y, YAO Y, MA L Q, YANG M, DING Y, SHEN X D. Synergistic effects in an AB_5/Co material as an anode for a secondary alkaline battery [J]. Int J Hydrogen Energy, 2010, 35: 4342−4346.

[8] LUAN B, CUI N, LIU H K, ZHAO H J, DOU S X. Effect of cobalt addition on the performance of titanium-based hydrogen-storage electrodes [J]. J Power Sources, 1995, 55: 197−203.

[9] ZHAO X Y, MA L Q, YAO Y, YANG M, DING Y, SHEN X D. Electrochemical energy storage of Co powders in alkaline electrolyte [J]. Electrochim Acta, 2010, 55: 1169−1174.

[10] CHUNG S R, WANG K W, PERNG T P. Electrochemical hydrogenation of crystalline Co powder [J]. J Electrochem Soc, 2006, 153: A1128−A1131.

[11] CHUNG S R, WANG K W, TENG M H, PERNG T P. Electrochemical hydrogenation of nanocrystalline face-centered cubic Co powder [J]. Int J Hydrogen Energy, 2009, 34: 1383−1388.

[12] LI L, WANGY P, WANG Y J, HAN Y, QIU F Y, LIU G, YAN C, SONG D W, JIAO L F, YUAN H T. Mesoporous nano-Co_3O_4: A potential negative electrode material for alkaline secondary battery [J]. J Power Sources, 2011, 196: 10758−10761.

[13] WANG Q H, JIAO L F, DU H M, SONG D W, PENG W X, SI Y C, WANG Y J, YUAN H T. Facile preparation and good electrochemical hydrogen storage properties of chain-like and rod-like Co−B nanomaterials [J]. Electrochim Acta, 2010, 55: 7199−7203.

[14] FERNANDES R, PATEL N, MIOTELLO A, JAISWAL R, KOTHARI D C. Stability, durability, and reusability studies on transition metal-doped Co−B alloy catalysts for hydrogen production [J]. Int J Hydrogen Energy, 2011, 36: 13379−13391.

[15] KRISHNAN P, ADVANI S G, PRASAD A K. Thin-film CoB catalyst templates for the hydrolysis of $NaBH_4$ solution for hydrogen generation [J]. Appl Catal B: Environ, 2009, 86: 137−144.

[16] WANG Q H, JIAO L F, DU H M, HUAN Q N, PENG W X, SONG D W, WANG Y J, YUAN H T. Investigation of novel cobalt-boron-carbon system as negative material for secondary alkaline battery [J]. Electrochim Acta, 2011, 58: 437−441.

[17] WANG Y, LEE J M, WANG X. An investigation of the origin of the electrochemical hydrogen storage capacities of the ball-milled Co−Si composites [J]. Int J Hydrogen Energy, 2010, 35: 1669−1673.

[18] WANG Q H, JIAO L F, DU H M, HUAN Q N, PENG W X, SONG D W, WANG Y J, YUAN H T. Comparison of Co−S electrodes synthesized via different methods for alkaline rechargeable batteries [J]. Electrochim Acta, 2011, 56: 4992−4995.

[19] WANG Q H, JIAO L F, DU H M, PENG W X, SONG D W, WANG Y J, YUAN H T. Facile synthesis and electrochemical properties of Co−S composites as negative materials for alkaline rechargeable batteries [J]. Electrochim Acta, 2011, 56: 1106−1110.

[20] HARAN B S, POPOV B N, WHITE R E. Studies on electroless cobalt coatings for microencapsulation of hydrogen storage alloys [J]. J Electrochem Soc, 1998, 145: 3000−3007.

[21] DURAIRAJAN A, HARAN B S, POPOV B N, WHITE R E. Cycle life and utilization studies on cobalt microencapsulated AB5 type metal hydride [J]. J Power Sources, 1999, 83: 114−120.

[22] CAO Y L, ZHOU W C, LI X Y, AI X P, GAO X P, YANG H X. Electrochemical hydrogen storage behaviors of ultrafine CoP particles prepared by direct ball-milling method [J]. Electrochim Acta, 2006, 51: 4285−4290.

[23] PENG W X, JIAO L F, HUAN Q N, LI L, YANG J Q, ZHAO Q Q, WANG Q H, DU H M, LIU G, SI Y C, WANG Y J, YUAN H T. Co_2P: A facile solid state synthesis and its applications in alkaline

rechargeable batteries [J]. J Alloys Compd, 2012, 511: 198−201.
[24] PRALONG V, DELAHAYE-VIDAL A, BEAUDOIN B, GÉRAND B, TARASCON J M. Oxidation mechanism of cobalt hydroxide to cobalt oxyhydroxide [J]. J Mater Chem, 1999, 9: 955−960.
[25] BARD A J, FAULKNER L R. Electrochemical method: Fundamentals and applications [M]. SHAO Yuan-hua, ZHU Guo-yi, DONG Xian-wei, ZHANG Bo-lin. Beijing: Chemical Industry Press, 2005: 262−270. (in Chinese)
[26] ZHAO X Y, MA L Q, DING Y, SHEN X D. Effect of particle size on the electrochemical properties of $MmNi_{3.8}Co_{0.75}Mn_{0.4}Al_{0.2}$ hydrogen storage alloy [J]. Int J Hydrogen Energy, 2009, 34: 3389−3394.
[27] SAKAIKE K, HIGASHI S, MURAKAMI H, MIYAZAKI S. Crystallization of amorphous Ge films induced by semiconductor diode laser annealing [J]. Thin Solid Films, 2008, 516: 3595−3600.
[28] ZHAO X Y, MA L Q, SHEN X D. Co-based anode materials for alkaline rechargeable Ni/Co batteries: A review [J]. J Mater Chem, 2012, 22(2): 277−285.
[29] YU Bin. Inorganic and analytical chemistry course [M]. Beijing, Chemical Industry Press, 2002: 242−243. (in Chinese)
[30] GAO X P, YAO S M, YAN T Y, ZHOU Z. Alkaline rechargeable Ni/Co batteries: Cobalt hydroxides as negative electrode materials [J]. Energy Environ Sci, 2009, 2: 502−505.

锗对 Ni/Co 电池负极材料链状 Co−P 电化学性能的影响

李佳佳[1]，赵相玉[1]，杜 伟[1]，杨 猛[1]，马立群[1]，丁 毅[1]，沈晓冬[1,2]

1. 南京工业大学 材料科学与工程学院，南京 210009；
2. 南京工业大学 材料化学工程国家重点实验室，南京 210009

摘 要：采用化学还原法制备链状 Co−P(4.9% P)合金粉末。将 Co−P 粉末与锗粉以不同质量比进行机械混合，形成 Co−P 复合电极。采用充放电测试和交流阻抗法研究锗对 Co−P 粉末电化学性能的影响。结果表明，加入锗粉后，复合电极的电化学性能显著提高。当 Co−P 合金粉与锗粉质量比为 5:1 时，电极的可逆放电容量为 350.3 mA·h/g，经 50 次循环后，容量保留率为 95.9%。从循环伏安曲线可看出，Co−P 复合电极主要发生 $Co/Co(OH)_2$ 转化。EIS 测试表明，混合电极(Co−P 合金粉与锗粉质量比为 5:1)的电荷转移电阻很低，表明锗的添加有助于促进 Co 氧化成 $Co(OH)_2$ 反应的进行。

关键词：Co−P 合金；锗；负极材料；电化学性能

(Edited by Xiang-qun LI)